Evaluation of Structure and Compressive Properties of Eco-friendly Cushioning Materials Based on Starch and Cellulose Types

Hae Min Jo,[a] Soo Hyun Lee,[a] and Ji Young Lee [b,*]

A reinforced eco-friendly cushioning material (ECM) comprising starch and cellulose material was developed. The ECM was prepared based on the starch type and cellulose material content; it was compared with commercial CMs. Different sizes of refined pulp (RP) and microfibrillated cellulose (MFC) were manufactured from hardwood bleached kraft pulp *via* beating and grinding, respectively. Thereafter, amylose-containing corn starch (CS) or amylopectin-only-containing glutinous rice starch (GS) was mixed with the manufactured cellulose materials. A slurry comprising starch and cellulose materials was homogenized for 2 min and lyophilized to prepare the ECM, after which the structure and strength characteristics of the prepared ECM were evaluated. The GS-prepared ECM produced a plate-like internal structure because of its amylopectin content, and amylose-containing CS exhibited a net-like shape. The cellulose materials offered support between starches with plate-like or net structure ECMs, and the pore shape was formed by adding MFC. As the cellulose material content increased, the strength of the ECM increased compared with that of the commercial CMs. Thus, ECMs with higher strength than their commercial counterparts could be manufactured with GS and cellulose materials.

DOI: 10.15376/biores.18.4.7839-7855

Keywords: Cushioning material; Starch; Amylopectin; Microfibrillated cellulose; Pulp; Loose-fill

Contact information: a: Department of Forest Products; b: Department of Environmental Materials Science/IALS, Gyeongsang National University, Jinju 52828, Republic of Korea;
** Corresponding author: paperyjy@gnu.ac.kr*

INTRODUCTION

Online shopping and delivery services have advanced significantly, and this progress has increased the importance of packaging technology and product protection. As consumers increasingly rely on the convenience of online shopping, the role of packaging in ensuring product safety during transportation has become ever more crucial (Meherishi *et al.* 2019; Gao *et al*. 2021; Debnath *et al*. 2022). Numerous consumers purchase food and consumables, as well as fragile items online; however, the values of such items, including those of electronics and glass, are considerably reduced by even the slightest damage (Kassim *et al*. 2023). Therefore, sellers have subscribed to using additional cushioning materials (CMs) inside packaging boxes to protect their products. CMs are manufactured in various purpose-dependent forms, ranging from relatively large molded foam to firmly hold the products in a box to small forms such as loose-fill foams to fill empty spaces (Nechita and Nastac 2022). The most widely utilized CMs include expanded polystyrene,

expanded polypropylene, expanded polyethylene (EPE), and expanded polyurethane (Liu *et al*. 2021; Li *et al*. 2022). These materials effectively absorb shocks due to their internal structures, which comprise numerous pores, as well as their controllable densities based on the foaming level (Amir *et al*. 2018; Nechita and Nastac 2022). However, petroleum-based expanded CMs are difficult to recycle (Tapia-Blacido *et al.* 2022); thus, they cause environmental issues at the manufacturing and disposal stages (Liu *et al.* 2021; Debnath *et al*. 2022). During the global shift towards sustainability, with the growth of online marketing and delivery services, it is crucial to produce eco-friendly CMs (ECMs) to reduce the utilization of synthetic polymers and ensure a sustainable packaging industry.

The most significant function of CMs is to offer protection to packaged goods during shipping. Therefore, they must exhibit suitable physical properties to control the impacts and vibrations that can be transmitted to the product during loading or transportation. An essential characteristic of cushion materials lies in their ability to dampen forces, absorb energy, and undergo deformation to minimize or prevent the transfer of energy or force to the packaged object. To fulfill its intended purpose, a cushion must possess the capacity to deform and effectively absorb energy. An extremely hard CM may not adequately absorb shocks of external impacts to the product or cause damage to the CM. Conversely, an extremely soft CM may be too weak to provide adequate cushioning properties, potentially failing to provide adequate protection upon small impacts from walls (floors). Therefore, ECMs must exhibit adequate flexibility and strength (Kang *et al*. 2010; Jiang *et al.* 2022).

Various materials have been proposed as ECMs that can satisfy the suitable properties of CMs, including polylactic acid composites or polyvinyl alcohol (PVOH) foams to replace plastic foams (Peelman *et al*. 2013; Oluwabunmi *et al*. 2020; Liu *et al*. 2021). Among the proposed alternative materials, expanded starch foams used in loose-fill foams have already become commercially available. Starch is the second most abundant natural polymer on earth; thus, it is a suitable and promising raw material to replace petroleum-based materials (Adigwe *et al.* 2022). To supplement the strength of starch loose-fill foams, adding various synthetic polymers or pre-treating starch have been proposed (Ghanbari *et al*. 2018). There have been attempts to improve the strength properties by diversifying starch raw materials obtained from cassava, potatoes, tapioca, and waxy corn or by controlling the foaming conditions (Georges *et al.* 2018; Pachor *et al*. 2019; Machado *et al.* 2020). Plasticizers, foam-control agents, and lubricants have been employed to facilitate extrusion and foaming. They include substances such as PVOH, fatty acid salts, amine salts, or paraffin wax (Nechita and Nastac 2022; Tapia-Blacido *et al*. 2022). Therefore, the manufacture of synthetic chemical-free ECMs to meet non-toxic and environmentally friendly demands is desired.

In this study, high strength ECMs comprising only starch and cellulose were manufactured. Like starch, cellulose is an environmentally friendly and highly abundant representative natural resource (Kadokawa *et al*. 2009; Li *et al.* 2021; Miranda-Valdez *et al*. 2023). To enhance the biodegradability of foamed plastics, ECMs were manufactured with cellulose material and combined cellulose fibers of different sizes to improve their strength. The two types of starch were chosen based on their composition and production quantity. Corn starch (CS) contains both amylose and amylopectin and is one of the most widely produced grains worldwide. Glutinous rice starch (GS), on the other hand, is primarily composed of amylopectin, suggesting that when used in the manufacturing of ECM, it is expected to exhibit different characteristics from corn starch. To manufacture

starch–cellulose ECMs under optimal conditions, the manufacturing characteristics using CS and GS were compared. Nanofibrillated cellulose exerts a high strength-improvement effect when utilized as an additive because of its high aspect ratio and fine fibrils (Gonzales-Ugarte *et al*. 2020; Barabanshchikov *et al*. 2021). Because of the high energy consumption and manufacturing cost of mechanical processing, this study used pulp fibers and microfibrillated cellulose (MFC) containing fine fibers (Kargupta *et al*. 2021; Pradhan *et al*. 2022). When manufacturing ECMs using cellulose raw materials and starch, it is anticipated that they will exhibit distinct structural characteristics, and differences based on the mixing ratios. Such variations are expected to have an impact on the compressive strength of ECMs. By selecting a very suitable starch type and adjusting the mixing ratio of the cellulose raw material, the possibility of replacing commercially available CMs was evaluated. As a result, we aimed to manufacture environmentally friendly ECMs for packaging based on the size of cellulose raw materials and the type of starch.

EXPERIMENTAL

Materials

GS and CS were employed for the manufacture of the ECM. The starches were supplied by Keundeul Food (Jinju, Republic of Korea) as dry powders. A hardwood bleached kraft pulp (HwBKP), which was supplied by Moorim Paper (Jinju, Republic of Korea), was used for the laboratory production of refined pulp (RP) and MFC. The starch–cellulose ECM that was prepared here was compared with the expanded CS (EC) (Fig. 1a) and EPE (Fig. 1b), which are commercial CMs with densities of approximately 30 kg/m^3.

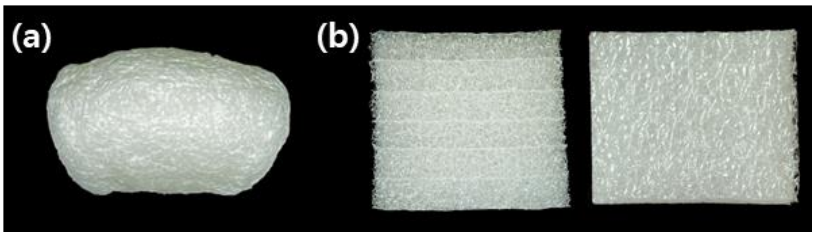

Fig. 1. Images of the commercial CMs (a: EC, b: EPE)

Preparation of the RP and MFC

RP and MFC were produced to prepare the starch–cellulose ECM. To prepare RP, HwBKP with a 1.57 wt % solid content was soaked in tap water and beaten to Canadian standard freeness (240 mL CSF) by a laboratory Hollander beater; the final concentration of RP after beating was 1.44 wt%. MFC was produced by beating and microgrinding, following the previously reported method (Park *et al*. 2020). Further, HwBKP was beaten to 450 mL CSF and diluted to 1.0% consistency for fibrillation. Thereafter, the pulp slurry with a 1.0 % solid content was fibrillated by a super mass colloider (MKZA6-2; Masuo Sangyo Co., Ltd., Kawaguchi, Japan) at 1,500 rpm. Next, the pulp slurry was fed into the grinder, and the fibrillation was performed once. Figure 2 shows RP and MFC preparation process.

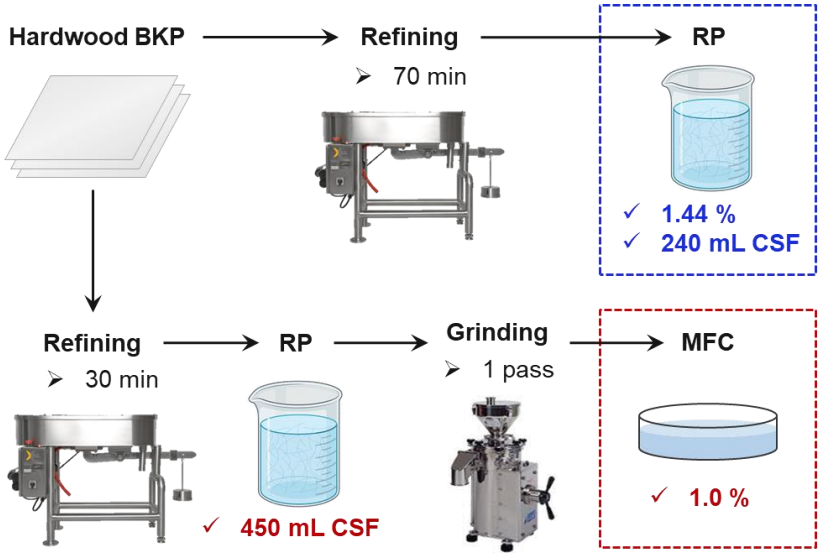

Fig. 2. Schematic diagram of RP and MFC preparation

Characterization of RP and MFC

The main properties of the cellulose materials were measured to compare the sizes of RP and MFC. The average fiber length, fiber width, and fines content of RP were measured using a fiber length analyzer (FQA-360; OpTest Equipment Inc., Hawkesbury, Canada). The fiber morphology was observed under an optical microscope (BX51; Olympus, Tokyo, Japan). Field emission scanning electron microscopy (FE-SEM; JSM-7610F; JEOL, Tokyo, Japan) was performed to observe the fiber morphology and fibrillation of MFC. To prepare a sample for FE-SEM imaging, the solvent was exchanged with ethyl alcohol (95%; Daejung Chemicals & Metals Co., Ltd., Siheung, Republic of Korea) and n-hexane (95%; Fisher Scientific, Waltham, USA). Before the imaging, sputter coating was performed using platinum, and the observation conditions included WD 6.0 mm in the solid electrolyte interface (SEI) mode, and the accelerating voltages were set to 5.0 kV. After capturing the FE-SEM images of the MFC, the fiber widths of 200 nanofibers were separately measured via image analysis using the three-dimensional (3D) image software (MP-45030TDI; JEOL, Tokyo, Japan).

Manufacture of the Starch–Cellulose ECM

Starch, RP, and MFC were used to manufacture the ECM. Different dosages of RP and MFC were added to the starch and mixed. The two types of starch (CS and GS) were individually gelatinized and used to manufacture the ECMs. Applying heat and moisture to starch granules causes them to swell, and the intermolecular bonds within the starch molecule break, resulting in the disruption of the crystalline structure (Chakraborty *et al*. 2022). Gelatinized starch, with its high moisture absorption capacity (Grundas 2003) and expanded state, is expected to maintain space within when dried. Therefore, to facilitate the gelatinization of starch, which had been diluted to a concentration of 3.5%, it was stirred for 30 min in a water bath at 80 °C. During gelatinization, water was added as needed to replace what was evaporated, maintaining a solids content of 3.5%. The gelatinized starch was used in the subsequent step while maintaining a temperature of 65 to 70 °C.

To prepare the starch–cellulose ECM, RP or MFC was added up to 30% of the total dry weight of the ECM, with the remaining composed of starch. The starch and cellulose

materials were mixed to ensure that the total dry fiber weight and density of ECM were 1.05 g and ~35 kg/m^3, respectively. Table 1 details the mixing conditions of starch and cellulose materials. The starch–cellulose mixture was homogenized for 2 min at 10,000 rpm using a homogenizer (HG-15A; Daihan Scientific, Republic of Korea), after which it was frozen at −30°C in a mold measuring 20 × 20 × 50 (mm). The frozen sample was lyophilized at −110°C for 48 h using a freeze dryer (HyperCOOL; Labogene, Lillerod, Denmark).

Table 1. Conditions for Manufacturing the Starch–Cellulose ECMs

Materials	Starch (wt %)	RP (wt %)	MFC (wt %)	Total (wt %)
RP	-	100	-	100
Starch	100	-	-	
GS + Cellulose	100	-	-	
	90	10	-	
	80	20	-	
	70	30	-	
	90	-	10	
	80	-	20	
	70	-	30	
CS + Cellulose	100	-	-	
	90	10	-	
	80	20	-	
	70	30	-	
	90	-	10	
	80	-	20	
	70	-	30	
GS + RP + MFC	70	25	5	
		20	10	
		10	20	
		5	25	

Morphology of the Starch–Cellulose ECM

The internal structure of the starch–cellulose material-composed ECM was investigated via SEM (JSM-6380; JEOL, Akishima, Japan). After cutting along the width direction with a stainless blade (ST-300; DORCO, San Diego, USA), the cross-section was observed. To prepare the specimen for SEM, sputter coating was performed with platinum, and the observation conditions were WD 11 mm in the SEI mode, and the accelerating voltage was 20 kV.

Physical Properties of the Starch–Cellulose ECM

The physical properties of ECMs are key to their ability to protect packaged goods from external impacts. To evaluate the flexibility and compression resistance of the ECMs, the compressive stress–strain of those that were manufactured according to the starch type and RP and MFC contents was measured with a universal strength tester (Universal Tester;

FRANK-PTI GmbH, Birkenau, Germany). All the fabricated specimens exhibited a size of 15 × 15 × 30 (mm). The force was measured up to a 10-mm strain corresponding to 1/3 of the length in three repeated tests. The measurement speed was at 10 mm/min, and the compression test was conducted between two plates used for measuring the ring crush compressive strength of the paper.

RESULTS AND DISCUSSION

Properties of HwBKP and MFC

Table 2 presents the fiber properties of cellulose materials. HwBKP was mechanically treated *via* refining for 70 min using a valley beater. As a result of the refining treatment, its fiber length and fiber width decreased, and its fines content increased. When pulp is used as a raw material for paper, its excessive fines content causes issues regarding dewatering (Seth 2003), although it can maintain the structure ECM during manufacturing. Figure 3 shows the fiber images and fiber width distributions of RP and MFC. MFC was divided into microsized fibers after one pass through the microgrinder (Figs. 3d and 3e).

Table 2. Fiber Characteristics of the Cellulose Materials

	Canadian standard freeness (mL CSF)	Fiber length (mm)	Fiber width (μm)	Fines content (%)
HwBKP	600	0.72	19.1	7.9
RP	240	0.37	18.5	35.1
MFC	-	-	0.27	-

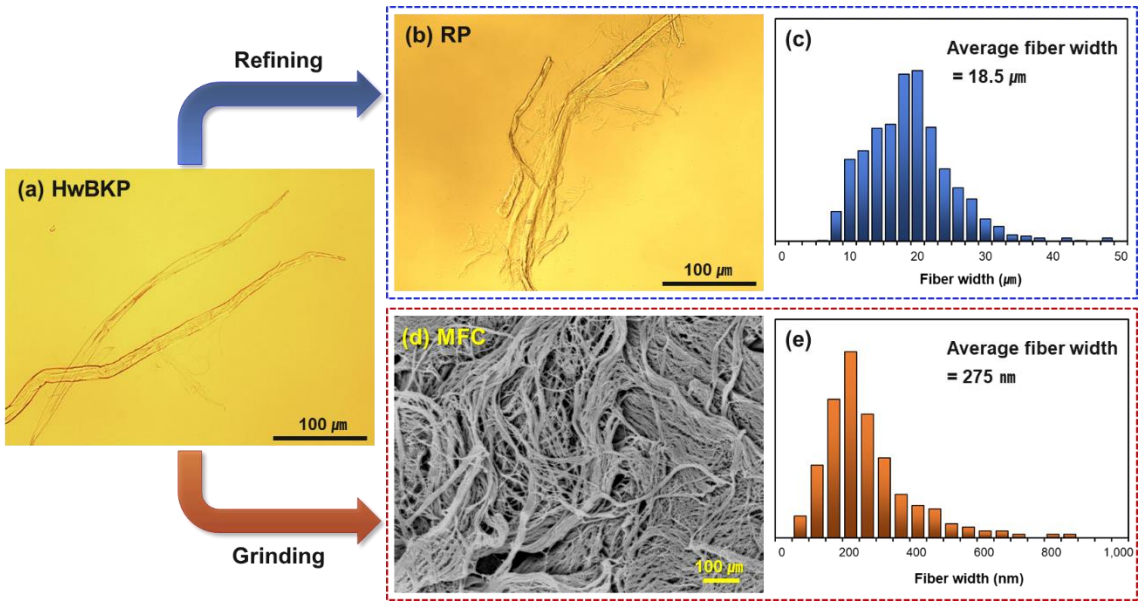

Fig. 3. Fiber morphology and fiber width distribution of the cellulose materials (a: HwBKP; b,c: RP; and d,f: MFC)

As the fiber length of MFC cannot be readily measured, the sizes of the two cellulose materials were compared *via* their fiber width. The average fiber width of MFC was 0.27 μm, and it consisted of fibers with a maximum size of ≤1 μm, while the fiber width of RP was distributed in the 8 to 50 μm range. RP was expected to form a large structure inside ECM and the fibrillated fiber combined with the starch and MFC. Considering that MFC contains numerous fine fibrils, the strength of the manufactured ECM can be increased via hydrogen bonding. Therefore, the two different sizes of cellulose materials can deliver different performances within the structure of the starch–cellulose ECM.

Structure of the Starch–Cellulose ECM

Figure 4 shows the SEM images of the internal structure of ECM comprising RP or starch only. The internal shapes of the ECMs that were manufactured from three types of raw materials differed in appearance. RP (Fig. 4a) was well-separated into individual fibers, and the two starch types exhibited completely different appearances (Figs. 4b–4c). GS comprising amylopectin exhibited a layered-plate shape, whereas CS with a high amylose content exhibited small and short interconnected structures. These characteristics of GS suggest the potential for forming an anisotropic structure in ECMs containing GS. The starch particles swelled and gelatinized when heated, following the penetration of water (Pither 2003). Generally, starch granules exhibit an oval or polyhedral shape (Domene-Lopez *et al*. 2019), although it is assumed that the granules are broken by homogenization to form a network by exposing the starch molecules. Several studies have reported that amylopectin and amylose exhibit a large-branched and small linear structure, respectively (Edwi 2019). Therefore, during the lyophilization of starch, CS with a high amylose content formed a short and dense network, and GS comprising only amylopectin formed a larger and wider layered network.

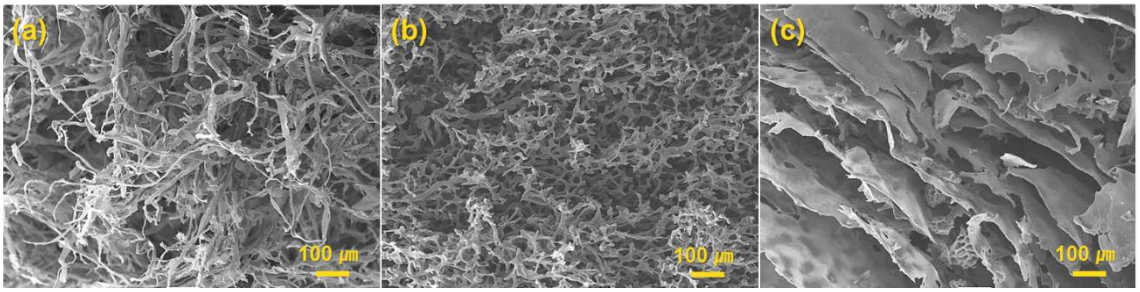

Fig. 4. SEM images of the ECM based on the utilized raw materials (a: RP, b: CS, c: GS)

Figures 5 and 6 show the internal and external morphologies, respectively, of the ECMs that were prepared from starch and RP. By mixing RP with starch, the shape of the bonding structure of ECM differed based on the starch type. GS helped to maintain the overall structure of the ECM. In Figs. 5a to 5c, CS combined with relatively large RP fibers to form a net structure, while GS formed a plate-like layer that was supported by the RP fibers (Figs. 5d to 5f). When starch and RP were mixed, the assembly form changed while maintaining the shape characteristics of each raw material without forming a new internal structure. The ECMs that were prepared from starch and RP formed a space inside, and a larger space was produced in the layer structure containing GS than in the network structure comprising CS. The GS-based ECM generated a large internal space *via* its plate-like layer

and RP support; its shape was maintained even with the increasing amount of RP. This structure can effectively improve flexibility and high strength when deformed by an external impact. Figure 6 shows the appearance of the starch-and-RP-mixed ECM. The external morphology differed with the starch type. Compared with the GS-based ECM, the CS-based one barely maintained its external shape, whereas the CS-based ECM sample shrank during freezing and drying, the GS-based one maintained its shape.

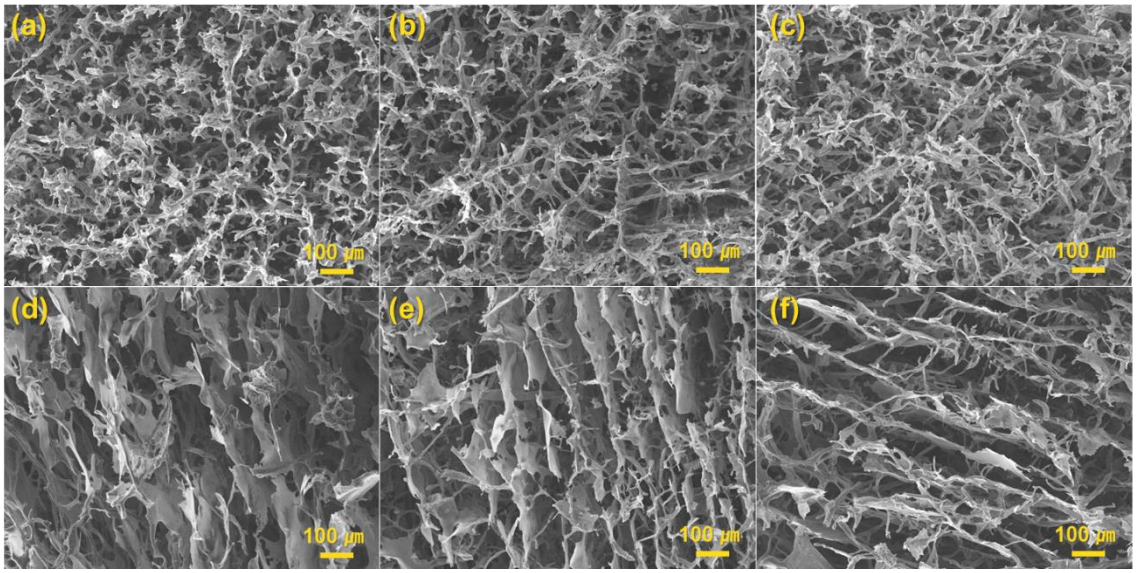

Fig. 5. SEM images of the CS-based ECMs depending on the RP contents (a: 10%, b: 20%, c: 30%) and GS-based ECM depending on the RP contents (d: 10%, e: 20%, f: 30%)

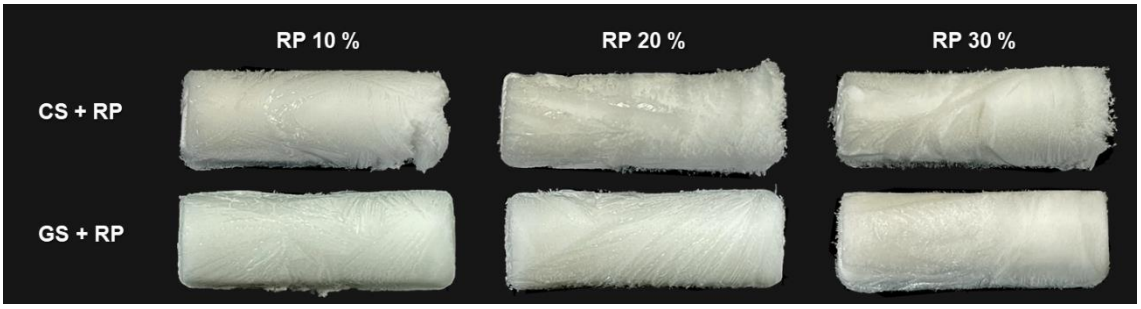

Fig. 6. External morphology of the ECMs composed of starch and RP

Figures 7 and 8 show the SEM images of the internal and external morphologies, respectively, of the ECMs that were prepared with starch and MFC. The images exhibited the internal spaces, although their shapes differed based on the starch type and MFC content. The network structures of CS and MFC were combined, and a hole was formed in the ECM that was prepared using 30% MFC (Figs. 7c and 7f). The GS maintained the plate-like layers just like when it was mixed with RP, and the MFC supported them between the layers. As the mixing ratio of MFC increased, an additional network was formed independently to create a wall. The ECM, which was prepared with 30% MFC, exhibited a noticeable pore morphology, although the size differed based on the starch type; the hole in the GS-based ECM was larger than that in the CS-based one. By assuming that all the specimens were fabricated using the same amount of dry fiber weight, the CS-based

ECM exhibited a higher density. Figure 8 shows the appearance of the MFC-containing ECM. As the MFC content increased, the shape of the CS-based ECM changed significantly, and a denser structure was formed inside the ECM (Fig. 7c). An increase in the bulk of the cushioning material and the formation of the hole structure inside the ECM can facilitate the absorption of external shocks, ensuring effective cushioning (Meherishi *et al*. 2019). Therefore, GS is more suitable than CS for the formation of large hole spaces inside ECM and maintenance of its external shape. Additionally, the different raw-material-dependent external and internal shapes influenced the subsequent physical properties of the materials.

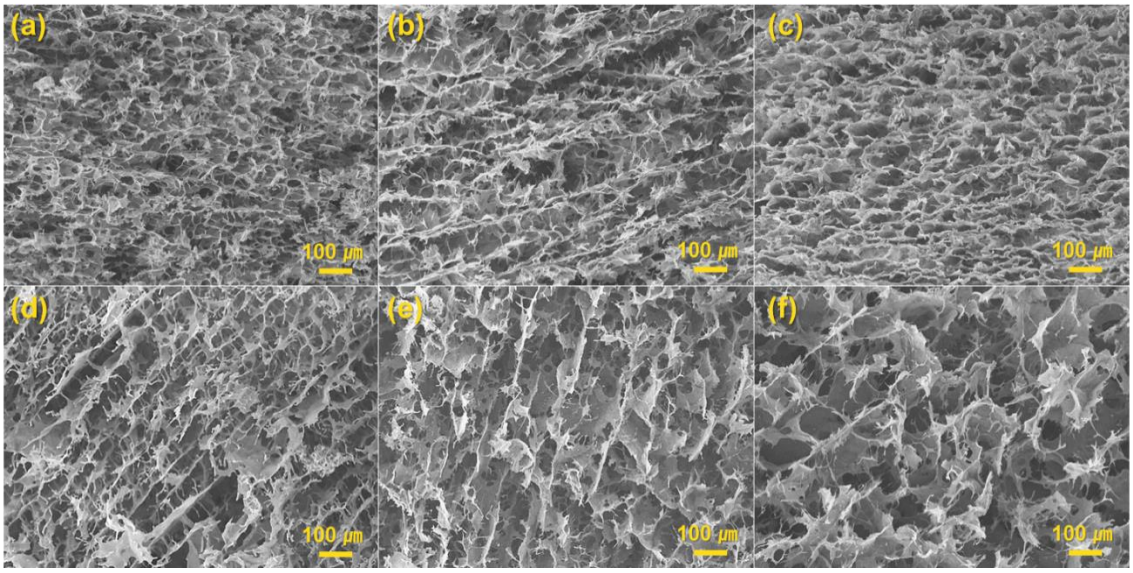

Fig. 7. SEM images of the CS ECM based on the MFC contents (a: 10%, b: 20%, c: 30%) and GS ECM based on the MFC content (d: 10%, e: 20%, f: 30%)

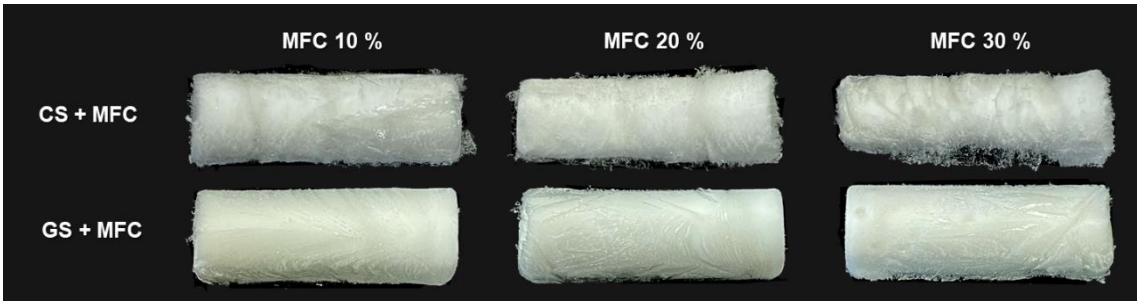

Fig. 8. External morphologies of the ECMs comprising starch and MFC

Figures 9 and 10 show the internal and external morphologies, respectively, of the ECMs that were prepared by mixing RP and MFC with GS. Dissimilar to the GS that facilitated the formation of the plate-like layer, the long RP facilitated the formation of a network structure, and the GS and MFC formed a plane that connected the fibers between them, thus filling the holes. The bonding of RP and MFC might have proceeded before that of starch and the cellulose materials because hydrogen bonding occurs more on the cellulose chains. As the MFC content increased, additional wall shapes were observed than individual fiber shapes, and it was possible to generate the shape of the pores and form

spaces inside the ECM (Figs. 9d and 9e). Although the mixing ratio of GS, RP, and MFC changed, the external shape was maintained stably (Fig. 10).

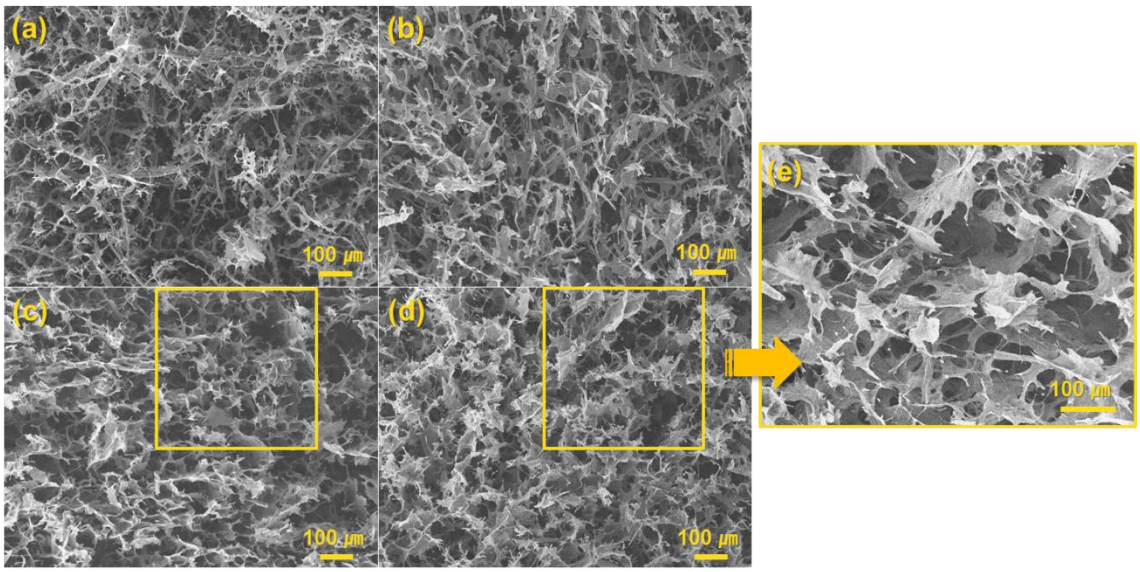

Fig. 9. SEM images of the GS ECM based on the RP and MFC contents (a: RP 25% + MFC 5%; b: RP 20% + MFC 10%; c: RP 10% + MFC 20%; d,e: RP 5% + MFC 25%)

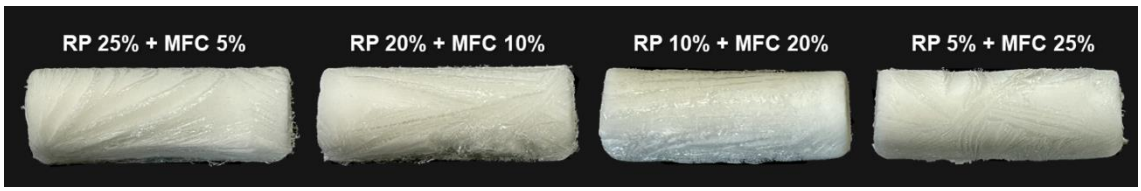

Fig. 10. External morphologies of ECMs composed of starch, RP, and MFC

Physical Properties of the Starch–Cellulose ECM

The load against deformation was measured (Figs. 11 and 12) to evaluate the physical properties based on the starch type and mixing ratio. When starch was mixed with RP or MFC, the strength increased significantly compared with the strength of starch only.

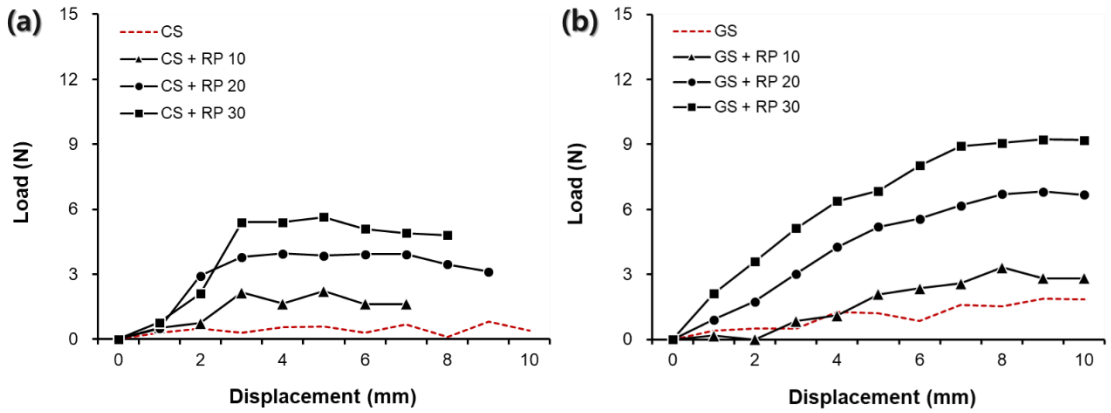

Fig. 11. Load-displacement curve of ECM containing RP (a: CS + RP, b: GS + RP)

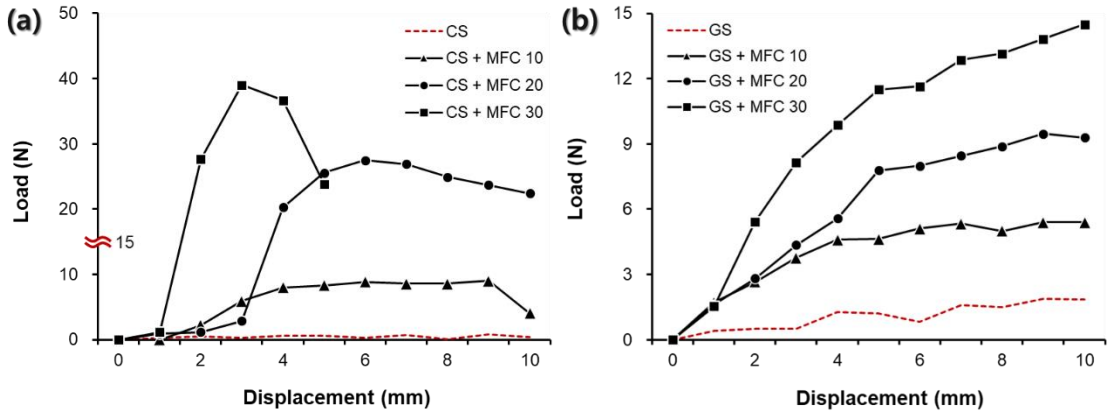

Fig. 12. Load-displacement curve of the ECM containing MFC (a: CS + MFC, b: GS + MFC)

As confirmed by the SEM image, the cellulose materials connected the network or plate-shaped structure of starch by supporting its internal structures. Put differently, the ECM was strengthened by changing the starch structure consisting of lines and planes formed into a 3D structure. Figures 11a and 12a reveal that the CS-based ECMs were relatively stiffer than the GS-based ones because the load resistance decreased sharply above a certain deformation level. This indicated that the CS-based ECM was not flexible and broke irreversibly over a certain deformation limit (Roberts and Holder 2011; Lee *et al*. 2014). Therefore, GS represented a more suitable starch type than CS as a cushioning material for shock absorption to protect packaged items during delivery.

Figure 13a shows the compressive stress–strain curve based on the starch type and mixing ratio with the cellulose materials. The strength of the ECM that was prepared by mixing GS, RP, and MFC was significantly higher than that prepared by mixing RP or MFC only. These results might be due to the different binding capacities of starch and cellulose. Starch is similar to cellulose in that it contains repeated glucose units, although in a different manner. Cellulose comprises β-1,4-glycosidic bonds that allow the linkage of molecules in a straight line, whereas starch does not (Wang *et al.* 2020). The α-1,4-glycosidic bonds in starch complicate its contact with other molecules by forming a loose helical structure, whereas the straight-chain structure of cellulose allows closer access or contact with other molecules, thereby easing hydrogen bonding (Shen and Gnanakaran 2009; Altaner *et al.* 2014; Zhang *et al*. 2021). Therefore, when the cellulose raw materials were added to GS together rather than separately, the addition facilitated the formation of an additional bond between RP and MFC, greatly improving the strength of the ECM. Even in the SEM image in Fig. 9, when RP or MFC was added to GS simultaneously rather than separately, the bonding between the cellulose materials was more evident, supporting the result in Fig. 12a. In the results based on the mixing ratio of RP and MFC (Fig. 13a), as the ratio of MFC increased, the strength and flexibility increased and decreased, respectively. As the MFC content of ECM increased, the flexibility decreased because of the increase in the formed networks between GS and the microfibril, and the internal structure became denser than that of ECM containing a high amount of RP. Therefore, the strength and flexibility of ECM can be controlled according to the mixing ratio of RP and MFC.

Figure 13b shows the compressive stress–strain curve of the commercial CMs. The plastic-based EPE was readily deformed and flexible, whereas EC broke at a certain

deformation limit. Several types of starch–cellulose ECMs prepared in this study resisted greater loads than their commercial counterparts without breaking. The ECM composed of GS, RP, and MFC exhibited a substantial load-bearing capacity, high strength, and a suitable level of flexibility.

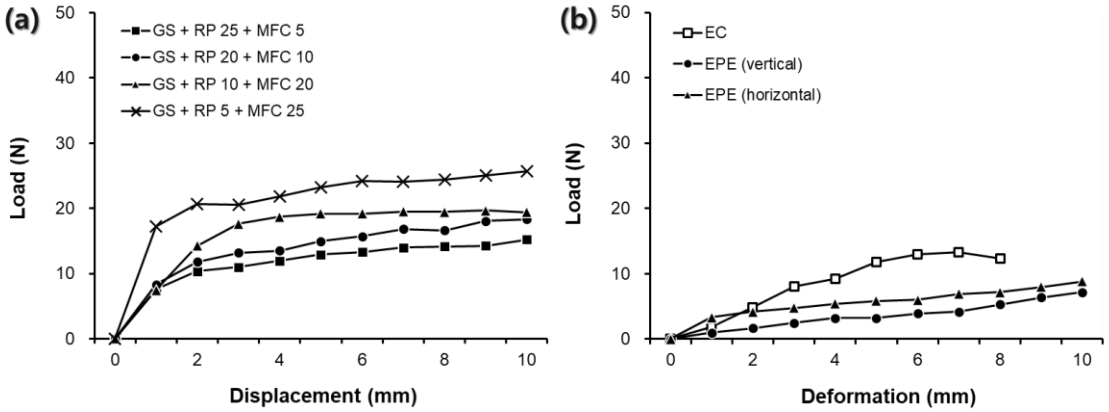

Fig. 13. Load-displacement curves of the ECMs (a: GS + RP + MFC, b: commercial CMs)

The Youngs' modulus was determined from the slope of the load-displacement curve and energy absorption from the area under the curve. (Table 3). The slope of the graph represents stiffness, indicating the resistance to deformation until specimen failure, while the area under the graph represents the energy absorbed by the specimen (Goodyear *et al*. 2011). When GS and CS were used alone, both the slope and area were lower under all conditions. However, when mixed with cellulose materials, both values increased. A greater slope in the graph signifies that a large force was detected with minimal deformation, confirming the production of a rigid ECM. A larger area does not necessarily imply higher strength or greater flexibility. ECMs based on CS were effective in increasing internal density, as observed in SEM images and external morphologies. Consequently, when mixed with different cellulose sources, they exhibited a sharp increase in slope. In contrast, GS-based ECMs, due to their larger internal pore size and spacing between starch layers, exhibited relatively more flexibility in compression when subjected to load.

When examining the differences based on cellulose materials, it was observed that the graph's slope increased more when MFC was mixed compared to RP, resulting in enhanced stiffness. This effect can be attributed to MFC's smaller size and higher microfibril content, which led to a denser internal structure when combined with starch, as illustrated in Figs. 5 and 7. When comparing relative differences based on slope and area, it is evident that specimens with GS 80% + RP 20% and CS 90% + MFC 10% exhibited similar areas, but the slope of the GS-based ECM was significantly lower. In such cases where the energy absorption capabilities of the ECMs were similar, this indicates that the CS-based ECM had higher stiffness. Additionally, the slope for GS 70% + MFC 30% was 1.92, whereas for CS 70% + RP 30%, the slope was 1.80, with the former having a considerably larger area. This suggests that while the initial stiffness of the ECMs was similar, specimens with a lower area tended to fail more rapidly.

Consequently, GS enables the production of ECMs with relatively lower stiffness compared to CS, yet with higher energy absorption capabilities. From the above results, it is evident that adjusting the content of starch and cellulose enables the production of ECMs

with the desired levels of stiffness and energy absorption. Therefore, in this study, it was possible to manufacture flexible and strong starch–cellulose ECMs with similar qualities to their commercial counterparts by replacing a part of starch with cellulose and mixing RP with MFC.

Table 3. Compressive Properties of Starch-Cellulose ECMs

Materials	Starch (wt %)	RP (wt %)	MFC (wt %)	Young's modulus (N/mm^2)	Absorbed energy (N·mm)
GS + Cellulose	100	-	-	0.30	10.6
	90	10	-	0.37	16.7
	80	20	-	0.84	43.8
	70	30	-	1.34	63.9
	90	-	10	1.12	40.9
	80	-	20	1.39	61.6
	70	-	30	1.92	95.3
CS + Cellulose	100	-	-	0.25	4.3
	90	10	-	0.72	10.5
	80	20	-	1.46	29.5
	70	30	-	1.80	34.1
	90	-	10	1.00	61.5
	80	-	20	4.58	165.0
	70	-	30	13.0	128.3
GS + RP + MFC	70	25	5	5.17	117.1
		20	10	5.89	138.1
		10	20	7.14	145.2
		5	25	17.23	214.1
Commercial CM	EC			2.16	74.3
	EPE (vertical)			0.72	34.8
	EPE (horizontal)			0.88	47.5

CONCLUSIONS

1. Eco-friendly cushioning materials (ECMs) prepared using only starch exhibited different internal structures based on the starch type. Amylose-containing corn starch (CS) formed a network structure, and the internal spaces in amylopectin-containing glutinous rice starch (GS) exhibited a plate-like structure.
2. ECMs comprising GS and cellulose materials formed pores via the interaction between the amylopectin-generated plate-like structure and cellulose-formed supporting network. Thus, it was possible to produce a strong internal structure while maintaining the bulk.

3. ECMs prepared with GS, refined cellulosic pulp (RP), and microfibrillated cellulose (MFC) were much stronger than that produced by only RP or MFC because of the improvement of the bonding strength between cellulose materials. This ECM exhibited higher physical properties than commercial EPE and EC.
4. It is possible to manufacture ECM with similar or higher qualities to those of commercial CMs using different sizes of GS and cellulose materials.

ACKNOWLEDGMENTS

This work was supported by the National Research Foundation of Korea (NRF) grant funded by the Korea government (MSIT) (No. NRF-2022R1A2C1007565).

REFERENCES CITED

Adigwe, O. P., Egharevba, E. O., and Emeje, M. O. (2022). "Starch: A veritable natural polymer for economic revolution," in: *Starch Evolution and Recent Advances*, Emeje, M. O., Blumenberg, M (eds.), IntechOpen, UK. DOI: 10.5772/intechopen.102941

Altaner, C. M., Thomas, L. H., Fernandes, A. N., and Jarvis, M. C. (2014). "How cellulose stretches: Synergism between covalent and hydrogen bonding," *Biomacromolecules* 15(3), 791-798. DOI: 10.1021/bm401616n

Amir, N., Hisham, M. S. M., and Abidin, K. A. Z. (2018). "Study of physical properties and shock absorption abilities of starch polymer foam as cushioning material for packaging," in: *MATEC Web of Conferences* 225(6), 06010. DOI: 10.1051/matecconf/201822506010

Barabanshchikov, Y., Phan, H, and Usanova, K. (2021). "Influence of microfibrillated cellulose additive on strength, elastic modulus, heat release, and shrinkage of mortar and concrete," *Materials* 14(22), article 6933. DOI: 10.3390/ma14226933

Chakraborty, I., Pooja, N., Mal, S. S., Paul, U. C., Rahman, M. H., and Mazumder, N. (2022). "An insight into the gelatinization properties influencing the modified starches used in food industry: A review," *Food and Bioprocess Technology* 15, 1195-1223. DOI:10.1007/s11947-022-02761-z

Debnath, M., Sarder, T., Pal, L., and Hubbe, M. A. (2022). "Molded pulp products for sustainable packaging: Production rate challenges and product opportunities," *Bioresources* 17(2), 39810-3870. DOI: 10.15376/biores.17.2.Debnath

Domene-Lopez, D., Garcia-Quesada, J. C., Martin-Gullon, I., and Montalban, M. G. (2019). "Influence of starch composition and molecular weight on physicochemical properties of biodegradable films," *Polymers* 11(7), article 1084. DOI: 10.3390/polym11071084

Edwi, T. M. Jr. (2019). "Starch: Granule, amylose-amylopectin, feed preparation, and recovery by the fowl's gastrointestinal tract," *Journal of Applied Poultry Research* 28(3), 566-586. DOI: 10.3382/japr/pfy046

Gao, Z., Dong, W., and Ji, Xiaomin. (2021). "Research on the reduction design of fragile product cushion packaging under the green development concept," in: *IOP Conf. Series: Earth and Environmental Science* 657, *2020 International Symposium on*

Energy Environment and Green Development, China, 012057. DOI: 10.1088/1755-1315/657/1/012057

Georges, A., Lacoste, C., and Damien, E. (2018). "Effect of formulation and process on the extrudability of starch-based foam cushions," *Industrial Crops and Products* 115, 306-314. DOI: 10.1016/j.indcrop.2018.02.001

Ghanbari, A., Tabarsa, T., Ashori, A., Shakeri, A., and Mashkour, M. (2018). "Thermoplastic starch foamed composites reinforced with cellulose nanofibers: Thermal and mechanical properties," *Carbohydrate Polymers* 197, 305-311. DOI: 10.1016/j.carbpol.2018.06.017

Gonzales-Ugarte, A. S., Hafez, I., and Tajvidi, M. (2020). "Characterization and properties of hybrid foams from nanocellulose and kaolin-microfibrillated cellulose composite," *Scientific Report* 10, article 17459. DOI: 10.1038/s41598-020-73899-z

Goodyear, S. R. and Aspden, R. M. (2011). "Mechanical properties of bone ex vivo," *Bone Research Protocols* 816, 555-571. DOI:10.1007/978-1-61779-415-5_35.

Grundas, S. T. (2003). "Wheat: Grain structure of wheat and wheat-based products," in: *Encyclopedia of Food Sciences and Nutrition*, Benjamin Caballero (eds.), Academic Press, USA, pp. 6137-6146. DOI:10.1016/B0-12-227055-X/01286-4

Jiang, S., Ding, M., Chen, W., and Wang, J. (2022). "Preparation and properties of flexible cushioning composites based on silicone rubber and warp-knitted spacer fabric," *Silicon* 14. DOI: 10.1007/s12633-022-02267-5

Kadokawa, J., Murakami, M., Takegawa, A., and Kaneko, Y. (2009). "Preparation of cellulose-starch composite gel and fibrous material from a mixture of the polysaccharides in ionic liquid," *Carbohydrate Polymers* 75(1), 180-183. DOI: 10.1016/jcarbpol.2008.07.021

Kang, Y., Zhang, D., and Du, H. (2010). "Air filled cushioning material, structures and properties," in: *Proceedings of the 17th IARPI World Conference on Packaging*, China, pp.1-4.

Kargupta, Wriju., Seifert, R., Martinez, M., Olson, J., Tanner, J., Batchelor, W. (2021). "Sustainable production process of mechanically prepared nanocellulose from hardwood and softwood: A comparative investigation of refining energy consumption at laboratory and pilot scale," *Industrial Crops and Products* 171, article 113868.

Kassim, N., Rahim, S. Z. A., Ibrahim, W. A. R. A. W., Shuaib, N. A., Rahim, I. A., Karim, N. A., Sandu, A. V., Pop, M. A., Titu, A. M., Bloch, K., and Nabialek, M. (2023). "Sustainable packaging design for molded expanded polystyrene cushion," *Materials* 16(4), article 1723. DOI: 10.3390/ma16041723

Lee, W. H., Kim, J. H., and Park, C. B. (2014). "Topology optimization for polymeric foam shock-absorbing structure using hybrid cellular automata," *International Journal of Automation Technology* 8(3), 365-375. DOI: 10.20965/ijat.2016.p0365

Li, T. T., Zang, K., Liu, P., Wang, Y. T., Hu, X., Wang, X., Lou, C. W., and Lin, J. H. (2022). "Construction of soft polyurethane cushioning composites based on integral fabric air layer: Reaching new levels in compression and cushioning behaviors," *Polymer Composites* 43(11), 8250-8258. DOI: 10.1002/pc.26996

Li, T., Chen, J., Brozena, A. H., Zhu, J. Y., Xu, L., Driemeier, C., Dai, J., Rojas, O. J., Isogai, A., Wagberg, L., and Hu, L. (2021). "Developing fibrillated cellulose as a sustainable technological material," *Cellulose* 590, 47-56. DOI: 10.1038/s41586-020-03167-7

Liu, B., Huang, X., Wang, S., Wang, D., and Guo, H. (2021). "Performance of polyvinyl alcohol/bagasse fibre foamed composites as cushion packaging materials," *Coatings* 11(9), article 1094. DOI: 10.3390/coatings11091094

Machado, C. M., Benelli, P., and Tessaro, I. C. (2020). "Study of interactions between cassava starch and peanut skin on biodegradable foams," *International Journal of Biological Macromolecules* 147, 1343-1353. DOI: 10.1016/j.ijbiomac.2019.10.098

Meherishi, L., Narayana, S. A., and Ranjani, K. S. (2019). "Sustainable packaging for supply chain management in the circular economy: a review," *Journal of Cleaner Production* 237, article 117582. DOI: 10.1016/j.clepro.2019.07.057

Miranda-Valdez, I. Y., Coffeng, S., Zhou, Y., Viitanen, L., Hu, X., Jannuzzi, L., Puisto, A., Kostiainen, M. A., Makinen, T., Koivisto, J., and Mikko, J. A. (2023). "Foam-formed biocomposites based on cellulose products and lignin," *Cellulose* 30, 2253-2266. DOI: 10.1007/s10570-022-05041-3

Nechita, P. and Nastac, S. M. (2022). "Overview on foam forming cellulose materials for cushioning packaging applications," *Polymers* 14(10), article 1963. DOI: 10.3390/polym14101963

Oluwabunmi, K., D'Souza, N. A., Zhao, W., Choi, T. Y., and Theyson, T. (2020). "Compostable, fully biobased foams using PLA and micro cellulose for zero energy buildings," *Scientific Reports* 10, article 17771. DOI: 10.1038/s41598-020-74478-y

Pachor, S., Sarkar, A., Dutta, A., Palanivelu, J., and Chidambaram, R. (2019). "Synthesis methods of starch-based polymer foams and its comparison with conventional polymer foams for food packaging applications," in: *Polymers for Agri-Food Applications*, Gutierrez, T. J (eds.), Springer, Germany, pp. 317-337. DOI: 10.1007/978-3-030-19416-1_16

Park, T. U., Lee, J. Y., Jo, H. M., and Kim, K. M. (2020). "Utilization of cellulose micro/nanofibrils as paper additive for the manufacturing of security paper," *Bioresources* 13(4), 7780-7791. DOI: 10.151376/biores.13.4.7780-7791

Peelman, N., Ragaert, P., De Meulenaer, B., Adons, D., Peeters, R, Cardon, L., Van Impe, F., and Devlieghere, F. (2013). "Application of bioplastics for food packaging," *Trends in Food Science & Technology* 32(2), 128-141. DOI: 10.1016/j.tifs. 2013.06.003

Pither, R. J. (2003). "Quality changes during canning," in: *Encyclopedia of Food Sciences and Nutrition*, Caballero, B (eds.), Academic Press, USA, pp. 845-851. DOI: 10.1016/B0-12-227055-X/00163-2

Pradhan, D., Jaiswal, A. K., and Jaiswal, S. (2022). "Emerging technologies for the production of nanocellulose from lignocellulosic biomass," *Carbohydrate Polymers* 285, article 119258. DOI: 10.1016/j.carbpol.2022.119258

Roberts, D. R. T., and Holder, S. J. (2011). "Mechanochromic systems for the detection of stress, strain and deformation in polymeric materials," *Journal of Materials Chemistry* 21(23), 8256-8268. DOI: 10.1039/C0JM04237D

Seth, R. S. (2003). "The measurement and significance of fines," in: *Pulp and Paper Canada-Ontario* 104(2), 41-44.

Shen, T., and Gnanakaran, S. (2009). "The stability of Cellulose: A statistical perspective from a coarse-grained model of hydrogen-bond networks," *Biophysical Journal* 96(8), 3032-3040. DOI: 10.1016/j.bpj.2008.12.3953

Tapia-Blacido, D. R., Aguilar, G. J., Andrade, M. T., Rodrigues-Juniro, M. F., and Guareschi-Martins, F. C. (2022). "Trends and challenges of starch-based foams for

use as food packaging and food container," *Trends in Food Science & Technology* 119, 257-271. DOI: 10.1016/j.tifs.2021.12.005

Wang, B. T., Hu, S., Yu, X. Y., Jin, L., Zhu, Y. J.., and Jin, F. J. (2020). "Studies of cellulose and starch utilization and the regulatory mechanisms of related enzymes in fungi," *Polymers* 12(3), 530. DOI: 10.3390/ppolym12030530

Zhang, C., Keten, S., Derome, D., and Carmeliet, J. (2021). "Hydrogen bonds dominated frictional stick-slip of cellulose nanocrystals," *Carbohydrate Polymers* 258, article 117682. DOI: 10.1016/j.carbpol.2021.117682

Article submitted: August 25, 2023; Peer review completed: September 8, 2023; Revised version received and accepted: September 24, 2023; Published: October 4, 2023.
DOI: 10.15376/biores.18.4.7839-7855